Characterisation of urea-denatured states of an immunoglobulin superfamily domain by heteronuclear NMR

ARTICLE *in* JOURNAL OF MOLECULAR BIOLOGY · JUNE 1998

Impact Factor: 4.33 · DOI: 10.1006/jmbi.1998.1702 · Source: PubMed

4 AUTHORS, INCLUDING:

Mark Bycroft
Medical Research Council (UK)
102 PUBLICATIONS **6,711** CITATIONS
SEE PROFILE

Stefan M V Freund
University of Cambridge
112 PUBLICATIONS **6,168** CITATIONS
SEE PROFILE

J. Mol. Biol. (1998) **278**, 417–429

JMB

Characterisation of Urea-denatured States of an Immunoglobulin Superfamily Domain by Heteronuclear NMR

Sun Fong, Mark Bycroft, Jane Clarke and Stefan M. V. Freund*

MRC Unit for Protein Function and Design Cambridge Centre for Protein Engineering, University Chemical Laboratory, Lensfield Road, Cambridge CB2 1EW UK

**Corresponding author*

The structural and dynamic properties of an immunoglobulin superfamily domain (IgSF), Ig 18′, have been characterised by NMR at 285 K, in the presence of 4.2 M and 6.0 M urea, respectively. Analysis of chemical shift deviations, $^{3}J_{HNH\alpha}$ coupling constants, sequential NOE pattern, and ^{15}N relaxation data reveals that although the two urea-denatured states are highly disordered, some local turn-like residual structures do exist. Moreover, some distinct differences between the properties of the two denatured states are observed. In 4.2 M urea-denatured Ig 18′, regions 80-83 and 86-92 adopt turn-like conformations, furthermore, region 84-93 is involved in slow exchange processes that occur on a micro- to millisecond time-scale. In the 6.0 M urea-denatured state, these turn-like conformations are less occupied, and chemical exchange processes in region 84-93 are largely reduced. In contrast, region 32-36 has persistent turn-like structures in both urea-denatured states. Some correlation between the spectral density function at 0 frequency, $J_{eff}(0)$, for the urea-denatured states and the secondary structure elements of the folded state have been observed. Except for the terminal regions, residues corresponding to β-strands have higher $J_{eff}(0)$ values compared to residues corresponding to loops. The characterisation and comparison of the two urea-denatured states highlight residues that possess properties that may be crucial for the initiation of folding of this domain.

Keywords: residual structure; I set; backbone dynamics; protein folding; β-sheet protein

Introduction

Located at the beginning of the folding reaction coordinate, highly disordered denatured states of proteins possess properties that may provide critical insight into the protein folding mechanism (Dobson, 1992; Moult & Unger, 1991). Although denatured states are inaccessible for detailed characterisation under conditions that favour the folded state, proteins in denaturing solvents may adopt properties similar to these states and have been the subject of increasing interest during the past few years (for reviews, see Shortle, 1993, 1996a). In studies of the denatured states of barnase (Arcus *et al.*, 1994, 1995; Freund *et al.*, 1996) and barstar (Wong *et al.*, 1996), some of the embryonic initiation sites, regions that possess persistent local residual structure, as determined by NMR methods, are found to be productive for protein folding. These regions contribute to tertiary interactions involved in the transition state of protein folding as derived from extensive protein engineering studies (Serrano *et al.*, 1992; Matouschek *et al.*, 1992; Nölting *et al.*, 1997).

Recent progress in NMR spectroscopy (Bax & Grzesiek, 1993; Kay, 1997; Zhang *et al.*, 1997). has rendered this technique a powerful tool for high-resolution characterisation of denatured proteins (e.g. see Neri *et al.*, 1992; Arcus *et al.*, 1994; Logan *et al.*, 1994; Wüthrich, 1994; Frank *et al.*, 1995;

Abbreviations used: NMR, nuclear magnetic resonance; 2D, two-dimensional; 3D, three-dimensional; TOCSY, total correlation spectroscopy; NOE, nuclear Overhauser enhancement; NOESY, nuclear Overhauser enhancement spectroscopy; HSQC, heteronuclear single quantum coherence; HMQC, heteronuclear multiple quantum coherence; CSA, chemical shift anisotropy; CPMG, Carr-Purcell-Meiboom-Gill sequence; ppm, parts per million.

0022–2836/98/170417–13 $25.00/0/mb981702

Wong *et al.*, 1996). The assignment of denatured proteins can be readily accomplished with triple resonance experiments, which enable the characterisation of structure and dynamics on a per residue basis. NMR characterisation of residual structure in denatured states has been based on various structural probes, such as chemical shift deviations (Barun *et al.*, 1994; Merutka *et al.*, 1995; Wishart *et al.*, 1995), amide hydrogen exchange (Roder, 1989; Radford *et al.*, 1992), coupling constants (Smith *et al.*, 1996), or qualitative distance information from NOEs (Zhang *et al.*, 1997). A semi-quantitative method that employs cross-relaxation rates (R_c) extracted from ^{15}N HSQC-NOESY-HSQC experiments for the detection of residual structure has been proposed (Freund *et al.*, 1996). Spectral density/reduced spectral density mapping (Farrow *et al.*, 1995; Ishima & Nagayama, 1995; Peng & Wagner, 1992a,b, 1995) has facilitated the analysis of heteronuclear NMR relaxation data. This approach is not limited by the need for a motional model and is an attractive means for describing the dynamics of denatured states.

Many studies have employed all-α or α/β proteins as models to investigate protein folding. Only recently have all-β proteins gained popularity as the subject of protein folding studies (Carlsson & Jonsson, 1995). The domination of long-range, non-local over short-range, local interactions in all β-sheet proteins has raised the question of how folding is initiated from an unfolded polypeptide chain. Theoretical studies suggest that the folding of all-β-sheet proteins may be initiated at β-hairpins (Finkelstein, 1991), which is supported by experimental results on tendamistat (Schönbrunner *et al.*, 1997). Alternatively, the hypothesis of a hydrophobic zipper mechanism (Dill *et al.*, 1993) has been supported by pulsed $H/^2H$ exchange studies on the folding of all-β interleukin-1β (Varley *et al.*, 1993).

Complete understanding of a protein folding mechanism requires characterisation of all important states along the folding reaction coordinate. This necessitates a detailed description of denatured state properties, including conformation of residual structure, internal dynamics, and persistence of these properties under different denaturing conditions. Our interest in the folding of β-sandwich proteins has prompted us to study the denatured state of Ig 18′, which is an immunoglobulin superfamily (IgSF) domain from the nematode *Caenorhabditis elegans* twitchin and contains no disulphide bond. Under non-denaturing conditions, Ig 18′ adopts a β-sandwich fold that has been classified to the I-set topology of the IgSF folds (Fong *et al.*, 1996). Here, we present NMR studies on the structural and dynamic properties of two urea-denatured states of Ig 18′. The differences between these denatured states and the potential implication for the folding of the protein are discussed.

Results

Urea-denaturation of Ig 18′ and HSQC spectra

$^1H,^{15}N$ HSQC spectra of Ig 18′ were acquired at pH 4.9 at different urea concentrations (1.5 M to 6.5 M) and at temperatures of 278 K to 298 K. Two sets of signals corresponding to the folded and denatured states were observed at low to intermediate urea concentrations. No folded signal was observed at urea concentrations >4.0 M. There is noticeable variation in the relative intensities of the $^1H,^{15}N$ HSQC cross-peaks with varying temperature and urea concentration. For instance, residues 85 to 93 show distinctly weaker intensities in 4.2 M urea than in 6.0 M urea at 285 K (Figure 1). This preliminary observation may indicate the presence of slow conformational exchange processes that moderate the dynamic behaviour of the denatured states. The intensity changes in the $^1H,^{15}N$ HSQC spectra with respect to temperature and urea concentration are largely reversible. Severe line-broadening was observed for the C-terminal region at higher temperatures. $^1H,^{15}N$ HSQC spectra were also acquired at protein concentrations of 1.6 mM, 0.8 mM and 0.4 mM at a urea concentration of 4.2 M. These spectra show identical chemical shifts and similar intensity variations for all residues, indicating that the differences between the 6.0 M and the 4.2 M urea spectra are unlikely to be caused by intermolecular interactions at the lower urea concentration. We report the detailed analysis at 285 K, at urea concentrations of 4.2 M and 6.0 M, under which most of the NMR signals were found to be quantifiable.

Deviation of chemical shifts from random coil values

The chemical shift deviations from random-coil values for 6.0 M urea-denatured Ig 18′ at 285 K were calculated based on sequence-corrected values for random-coil peptides (Barun *et al.*, 1994; Wishart *et al.*, 1995). Most of the backbone chemical shifts show no significant deviations from these values. Significant deviations (>2 ppm for ^{15}N shifts; >0.6 ppm for $^{13}C^{\alpha}$ shifts; >0.4 ppm for ^1H amide shifts; >0.1 ppm for H^{α} shifts) were observed for residues Leu6, H^{α}; Ile14, N; Pro32, C^{α}; Thr33, N; Ala34, HN; Trp36, H^{α}; Ser41, C^{α}; Ser56, H^{α}; Thr57, H^{α}; Glu89, C^{α}. A similar pattern for the chemical shift deviations was observed for the spectra recorded at 4.2 M urea (Figure 2). The pattern of the chemical shift deviations for different nuclei suggest that region 32-36 may contain some non-random local conformation in both denatured states.

$^3J_{HNH\alpha}$ coupling constants

The $^3J_{HNH\alpha}$ coupling constants were determined for Ig 18′ in 4.2 M and in 6.0 M urea at 285 K (Figure 3) by the method of Stonehouse & Keeler

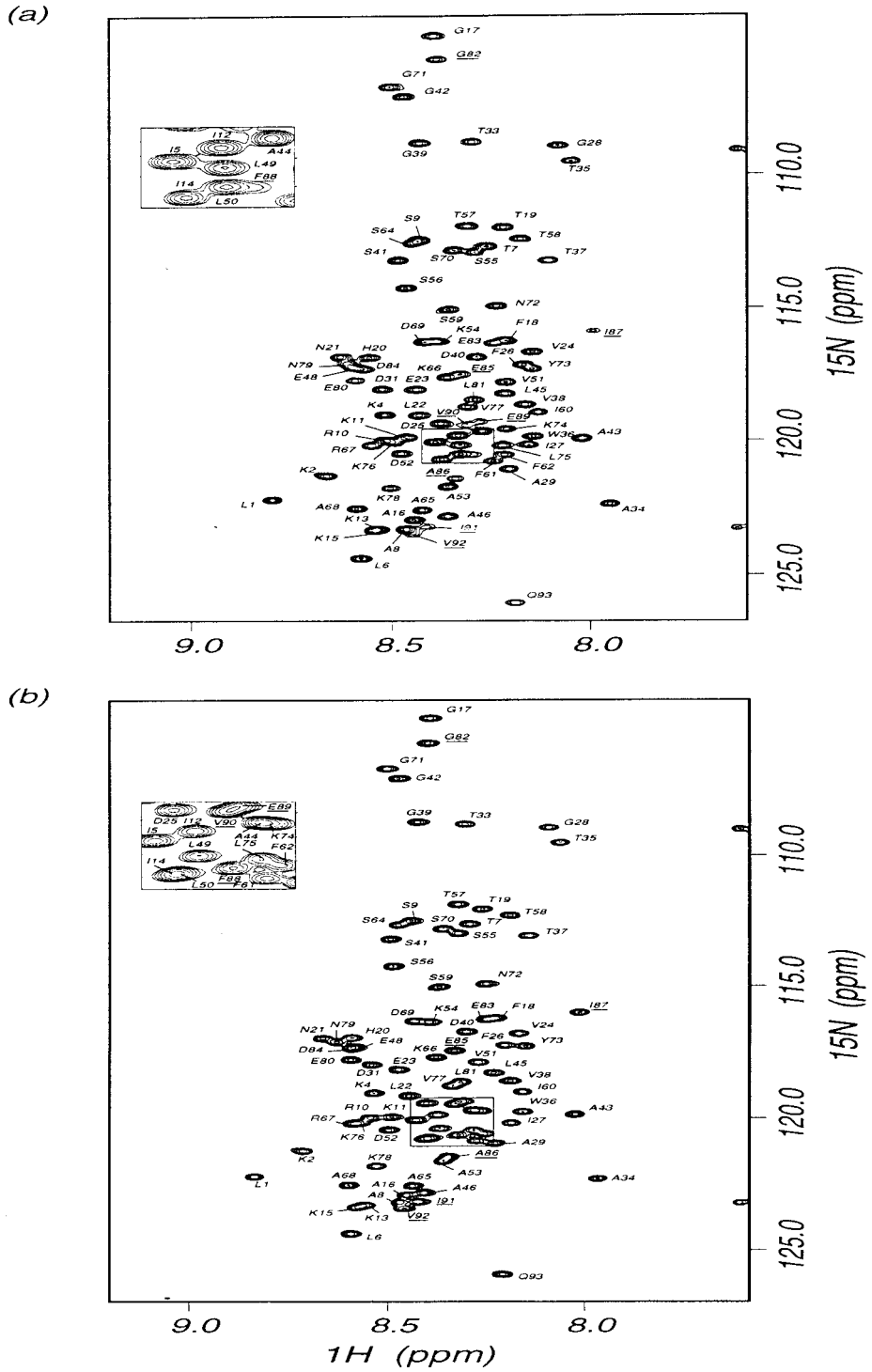

Figure 1. ^{1}H, ^{15}N HSQC spectra of Ig 18′ at 285 K in (a) 4.2 M urea and (b) 6.0 M urea. Assignments are indicated with the one-letter code. The boxed regions are enlarged and shown in the insets. Some of the residues that show distinctive intensity differences in the two spectra are underlined.

(1995). In general, the mean values for each amino acid residue type were close to those reported in the literature for denatured proteins (Arcus *et al.*, 1995; Smith *et al.*, 1996; Wong *et al.*, 1996). Compared with previously reported random coil model $^{3}J_{HNH\alpha}$ values from the ALL parameter set (Smith *et al.*, 1996), residues that have non-negligible deviations ($> \pm 0.7$ Hz) from these values are: Asp31, Thr33, Val38, Leu75 and Ala86 for Ig 18′ in 4.2 M urea and Thr7, Asp31, Thr35, Thr58 and Glu89 for Ig 18′ in 6.0 M urea.

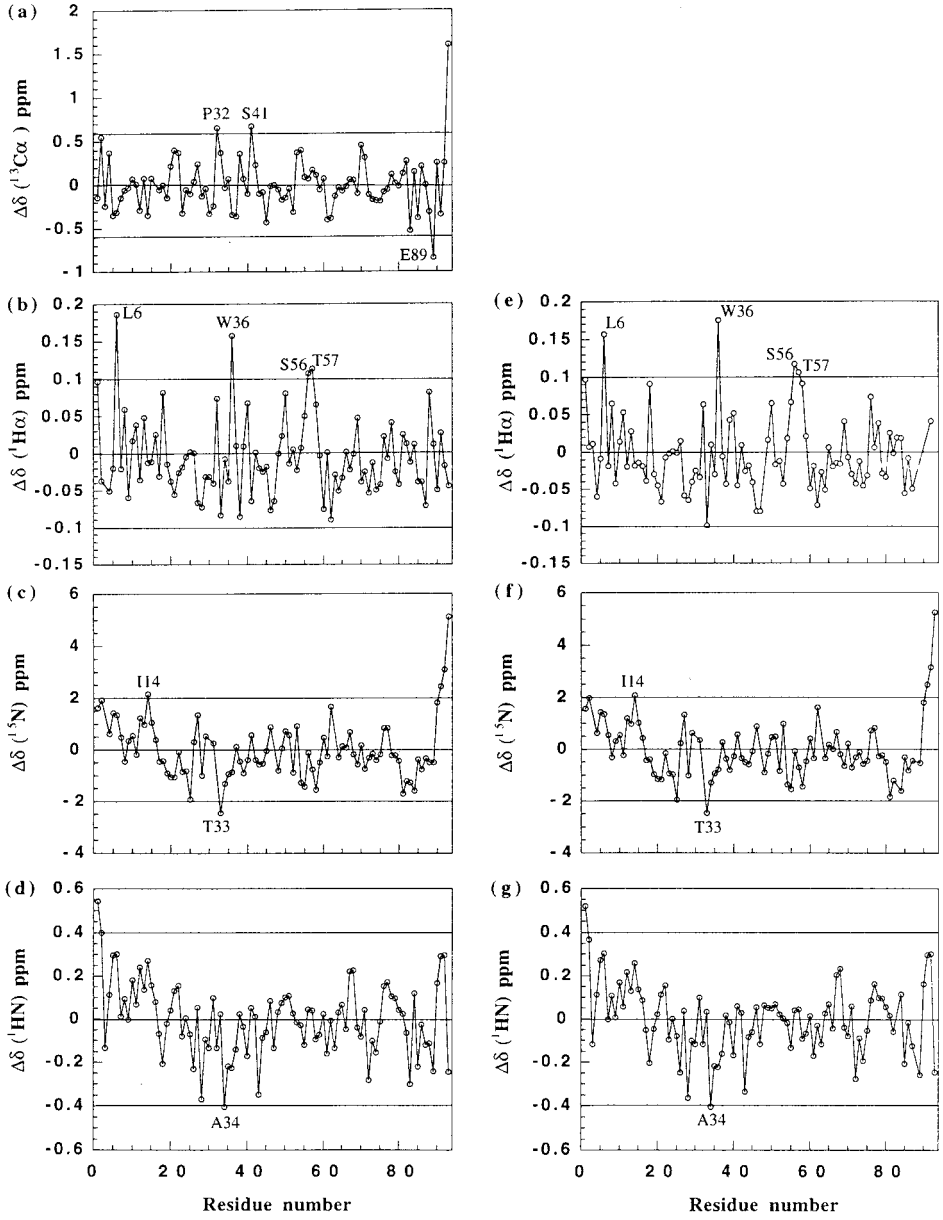

Figure 2. Chemical shift deviations (Δδ) from random coil values for backbone resonances of twitchin Ig 18′ in 4.2 M and 6.0 M urea: (a), (b), (c) and (d) are observed in 6.0 M urea at 285 K; (e), (f) and (g) were obtained in 4.2 M urea at 285 K. Sequence-corrected ^{15}N random coil shifts were used (Barun *et al.*, 1994). The ^{1}H and ^{13}C chemical shift deviations for residues that are immediately followed by proline in the sequence were further corrected in the analysis (Wishart *et al.*, 1995). Random coil chemical shifts for ^{1}H and ^{13}C resonances were taken from Wishart *et al.* (1995). Residues with significant chemical shift deviations (>2 ppm for ^{15}N; >0.6 ppm for $^{13}C^{\alpha}$; > 0.4 ppm for ^{1}HN; > 0.1 ppm for $^{1}H^{\alpha}$) are labelled.

$d_{NN(i,i+1)}$ NOE analysis

The nuclear Overhauser enhancement (NOE), with its r^{-6} distance dependency, has the highest sensitivity to detect minor populations of conformers that have structural elements that bring protons into close proximity. Previous studies have shown that, in particular, the ^{15}N,^{1}H,^{15}N HSQC-NOESY-HSQC experiment is a valuable tool for analysis of denatured proteins due to its excellent signal dispersion and high sensitivity (Freund *et al.*, 1996; Wong *et al.*, 1996). σ_{NN} values (the ratio of the lineshape-fitted intensities of the $d_{NN(i,i+1)}$ NOE cross-peak to the diagonal-peak) extracted from ^{1}H,^{15}N HSQC-NOESY-HSQC experiments can be used as semi-quantitative probes for the detection of residual structure (Wong *et al.*, 1996). Alternatively, σ_{NN} values can be converted to cross-relaxation rates, R_c (Esposito & Pastore, 1988; Macura & Ernst, 1980), which are normalised according to their mixing time (see Materials and Methods). The correlation between residual struc-

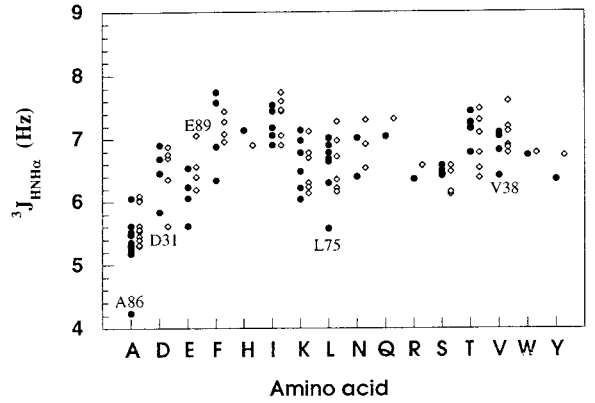

Figure 3. Plot of $^3J_{HNH\alpha}$ coupling constants against amino acid type. Filled circles and open diamonds indicate 4.2 M and 6.0 M data, respectively. The one-letter code is used to denote the amino acid type. Some of the residues that deviate significantly from random coil values (Smith *et al.*, 1996) are labelled.

ture as assigned based on primary sequence-dependent R_c rates and potential initiation sites as deduced from protein engineering studies has been established for barnase (Freund *et al.*, 1996).

In Ig 18′, 80% of the $d_{NN(i,i+1)}$ NOEs can be quantified for the 4.2 M and the 6.0 M urea denatured states at 285 K (Figure 4). High R_c values are found for Ala34 and Trp36 under both conditions, whereas only the denatured state at 4.2 M urea exhibits high R_c values for residues 80 to 90. For the denatured state at 6.0 M urea, these residues exhibit average R_c values. An increase in R_c implies that either the region has shorter H_N-H_N distances and/or the region is experiencing local restrictions of backbone motion.

$\sigma_{N\alpha}/\sigma_{\alpha N}$ NOE ratio analysis

The $d_{\alpha N(i+1,i+1)}$:$d_{\alpha N(i,i+1)}$ NOE ($\sigma_{N\alpha}/\sigma_{\alpha N}$) ratios (Figure 5) were derived from 3D ^{1}H,^{15}N NOESY-HMQC spectra recorded with a mixing time of 250 ms. However, as a result of poor dispersion of the H^α resonances, ratios for only about half of the residues were obtained. Note that the $\sigma_{N\alpha}/\sigma_{\alpha N}$ values for the majority of residues in the regions that display large R_c values (residues 34 to 36 and 85 to 90) could not be determined due to either severe overlap or missing signals, in particular for the 4.2 M urea data. The patterns observed for both urea concentrations are very similar and show some degree of variation across the sequence in the $\sigma_{N\alpha}/\sigma_{\alpha N}$ range of 0.15 to 0.56. Apart from the fact that lower values are observed at the N-terminal region, no obvious trend can be inferred from these data.

Reduced spectral density functions

Spectral density functions at 0 ($J_{eff}(0)$), ω_N (J(50 MHz)), and $\omega_H + \omega_N$ (J(450 MHz)) were calculated for both urea-denatured states from ^{15}N relaxation data at 11.74 T based on the reduced spectral density mapping approach (Figure 6). In general, an increase in $J_{eff}(0)$ (see Materials and Methods for a definition of $J_{eff}(0)$) is accompanied by an increase in the corresponding J(50 MHz) and a decrease in J(450 MHz) values. The spectral density functions at different frequencies have similar values for both denatured states, except for the values of $J_{eff}(0)$ in region 84-93, which are significantly higher in 4.2 M urea.

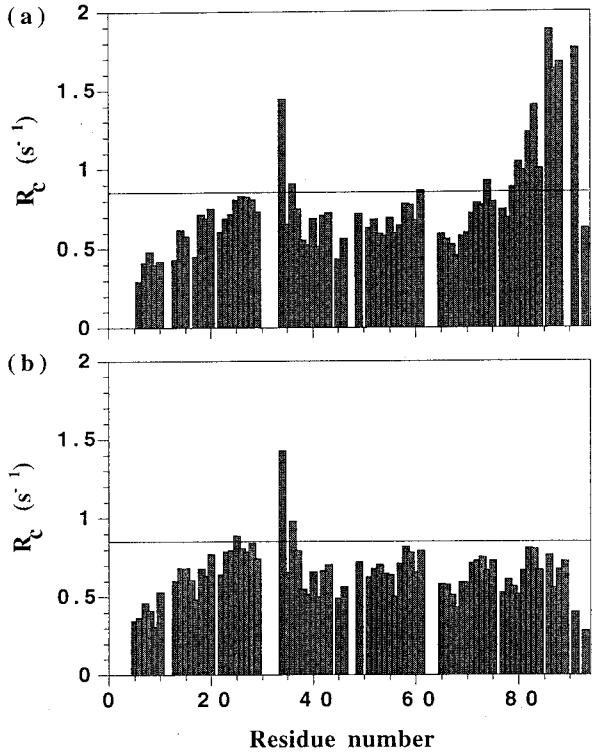

Figure 4. R_c observed for Ig 18′ in (a) 4.2 M and (b) 6.0 M urea. Values were derived from 3D ^{1}H,^{15}N HSQC-NOESY-HSQC spectra recorded with a 250 ms mixing time. The value of average R_c plus one standard deviation for the 6.0 M data is indicated with the horizontal lines in the plots.

Interestingly, the pattern observed for $J_{eff}(0)$ roughly follows the secondary structure of folded Ig 18′: ''peaks'' observed in the $J_{eff}(0)$ plots correspond to β-strand regions of the folded protein, whereas ''troughs'' correspond to loop regions.

As $J_{eff}(0)$ in region of 84-93 is substantially higher for Ig 18′ in 4.2 M urea than in 6.0 M urea, but no corresponding change is observed for J(50 MHz) or J(450 MHz), it is most likely that the enhancement in $J_{eff}(0)$ is a result of contributions from chemical exchange processes. This is supported by studies of the dependency of transverse relaxation rate R_2 on the spin-echo refocussing delay length in experiments based on the CPMG sequence. Substantial dependencies of the R_2 values on the spin-echo refocussing delays are observed for residues Ala29,

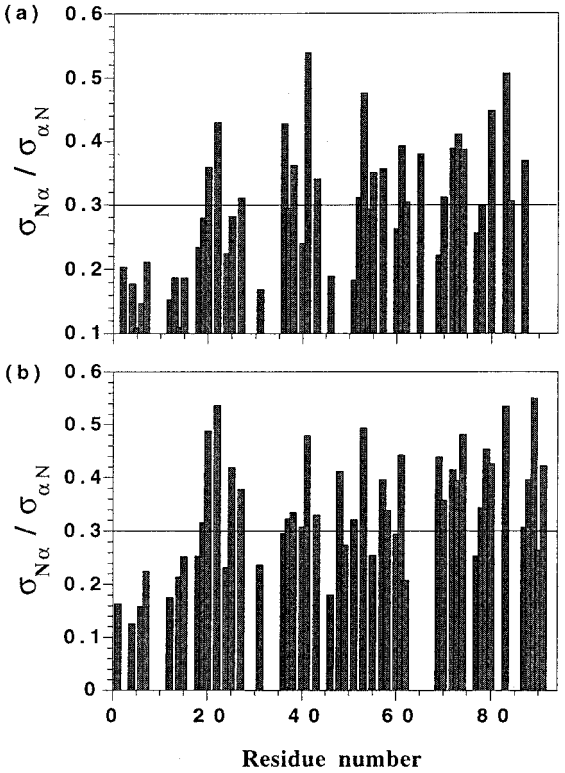

Figure 5. $\sigma_{N\alpha}/\sigma_{\alpha N}$ ratio for Ig 18′ in (a) 4.2 M urea and (b) 6.0 M urea. $\sigma_{N\alpha}/\sigma_{\alpha N}$ were determined as the intensity ratio of $H^{\alpha}(i+1)$-HN$(i+1)$ to $H^{\alpha}(i)$-HN$(i+1)$ NOEs derived from 3D ^{1}H, ^{15}N NOESY-HMQC spectra with a 250 ms mixing time. The predicted $\sigma_{N\alpha}/\sigma_{\alpha N}$ ratio for extended conformations (Saulitis & Liepins, 1990) is indicated by the horizontal lines.

Tyr73, Ala86, Ile91 and Val92 in 4.2 M urea, and Lys66 in 6.0 M urea, indicating significant contributions from chemical exchange to these residues.

Discussion

Equilibrium urea denaturation of Ig 18′, monitored by both fluorescence and far UV CD, can be accounted for by a two-state process in which only the folded and the denatured states are populated (Fong *et al.*, 1996). Our NMR results agree with these studies, as only two sets of signals corresponding to the folded and the denatured states are observed under conditions where denaturation is not complete. The denatured state of a protein is an ensemble of interconverting conformers (Dobson, 1992; Shortle, 1996b). This description raises fundamental questions concerning structural features of conformers present and their rates of interconversion. Particular regions in a denatured protein may have different rates of interconversion possibly caused by preferences for certain local conformations. This might be important for an understanding of denatured states and may provide insight into the protein folding mechanism.

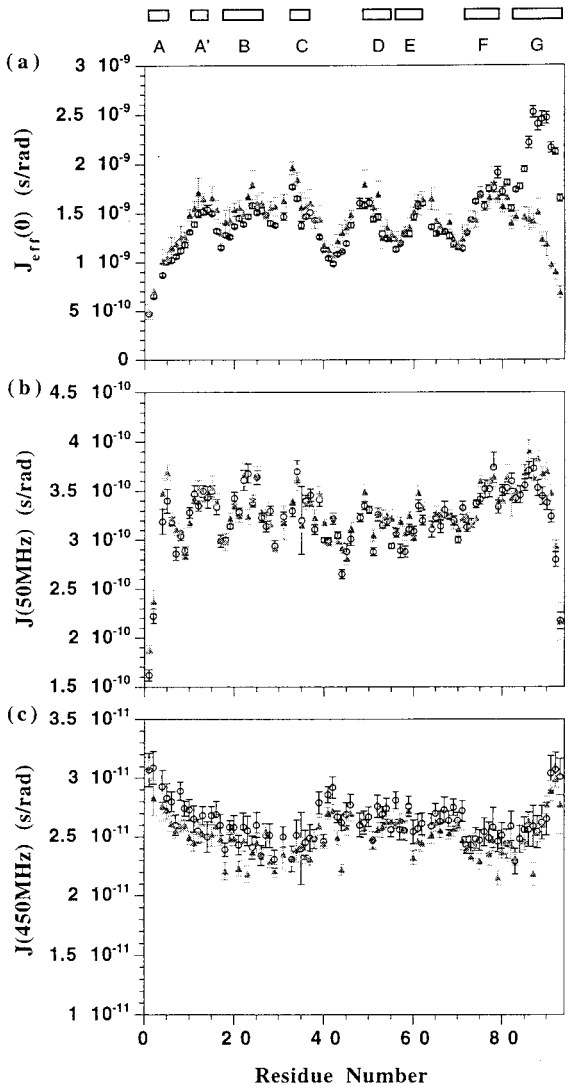

Figure 6. Spectral density functions of Ig 18′ at (a) 0, (b) 50 and (c) 450 MHz derived at 11.74 T in 4.2 M urea (open black circles) and in 6.0 M urea (filled grey triangles). The β-strand regions in folded Ig 18′ are shown as open bars at the top of the Figure. Standard deviations are shown as error bars.

Only one set of signals for Ig 18′ was observed in the ^{1}H,^{15}N correlation spectra at 285 K, pH 4.9 and urea concentrations of 4.2 M and 6.0 M. This indicates that only the denatured states are populated under these conditions, and that the interconversion between the denatured conformers is on an intermediate to fast NMR time-scale ($\geqslant 10^{3}$ s^{-1}). The NMR spectra are characterised by limited dispersion close to random coil values, which is indicative of a high degree of disorder. All experimental observables are ensemble averaged and biased by the large population of ''random coil'' conformers to various extents. The contribution from structured conformers is thus best described by a combinatorial analysis of chemical shifts, coupling constants, NOEs, and their deviations

from random coil or baseline values. On the other hand, relaxation data can provide complementary insight into the mobility of the ensemble of polypeptides on a pico-to millisecond time-scale, which may reflect the heterogeneity in different regions of the denatured polypeptide with respect to the rates of interconversion between local conformations.

Distinctive backbone dynamic patterns are observed for the urea-denatured states of Ig 18′

The typical value of the $\{^1H\text{-}^{15}N\}$ NOE for a rigid folded protein is around 0.8 (Kay *et al.*, 1989). The average $\{^1H\text{-}^{15}N\}$ NOEs observed for the two urea-denatured states of Ig 18′ are about 0.1, which indicates that the denatured states are highly flexible.

Inspection of the sequence dependence of $J_{eff}(0)$ on the urea-denatured states reveals some correlations with secondary structure elements of the folded state (Figure 6). Residues corresponding to β-strands have higher $J_{eff}(0)$ values compared to residues corresponding to loops (except for the terminal regions). One possible explanation for this observation is an equilibrium on an intermediate to fast time-scale between a small population of folded state and the denatured state, which would result in chemical exchange contributions to $J_{eff}(0)$ for all residues. This folding-unfolding equilibrium should be sensitive to a change in the denaturant concentration. Most of the $J_{eff}(0)$ values of the 6.0 M urea-denatured state are identical with or only marginally higher than the values observed for the 4.2 M urea denatured state. This supports the interpretation that these variations are associated with the intrinsic motional properties of the denatured state.

The $J_{eff}(0)$ values from the 6.0 M urea data are slightly higher than those from the 4.2 M data, while the reverse is observed for the J(450 MHz) values. This can be attributed to the more viscous nature of the 6.0 M urea solution, which shifts the distribution of the spectral density function of the protein towards lower frequencies. By varying the spin echo refocussing delays in CPMG experiments, we observe that, except for region 84-93 in 4.2 M urea, which shows significant exchange contributions, average exchange contributions to R_2 at a lower bound rate of approximately 100 to 1000 s^{-1} (assuming two-site exchange) are less than 10% in the two denatured states, which is within experimental error and may not be significant (data not shown). The terminal residues (1 to 4 and 91 to 93) are subject to fast motions occurring on a nano- to sub-nanosecond time-scale, as judged from the shift of the frequency distribution of the spectral density function to higher frequencies resulting in an increase of J(450 MHz) and a decrease of J(50 MHz). This is also observed for region 39-44, where a substantial decrease in $J_{eff}(0)$ is accompanied by decrease in J(50 MHz) and increase in J(450 MHz).

It can be inferred that the 4.2 M and the 6.0 M urea-denatured states of Ig 18′ experience motional restriction in regions: 13-16, 23-27, 31-36, 48-52, 60-64 and 73-81 (Figure 6). They include motions on a nanosecond time-scale and some of them may be associated with chemical exchange processes on a micro- to millisecond time-scale. In addition, region 84-93 of Ig 18′ in 4.2 M urea experiences substantial chemical exchange, which dramatically increases the $J_{eff}(0)$ values but does not lead to an increase in J(50 MHz) or decrease in J(450 MHz). Chemical exchange in this region is largely reduced in 6.0 M urea.

Turn-like transient structures are observed in urea denatured Ig 18′

The correlation between chemical shift deviations and the $^3J_{HNH\alpha}$ data suggests that region 31-36, which corresponds to the B-C turn and part of the C-strand of the folded state, may have non-random local structure in 4.2 M and 6.0 M urea. This structure is probably turn-like, as inferred from the lower $^3J_{HNH\alpha}$ values. This is supported by higher R_c values observed for Ala34 and Trp36, which indicate a decrease in the $H_N\text{-}H_N$ distances and/or a decrease in the mobility of the $H_N\text{-}H_N$ pairs in this region (equation (6)). In an attempt to separate the dynamic contribution to R_c from the $H_N\text{-}H_N$ distance contribution, we assume that $J(0)$ of $H_N\text{-}H_N$ pairs is proportional to $J_{eff}(0)$ of individual HN vectors. R_c values are then normalised against their corresponding $J_{eff}(0)$ values. The resulting $R_c/J_{eff}(0)$ ratio can be used as a parameter for a qualitative comparison of the $H_N\text{-}H_N$ distances in the denatured states (Figure 7). A higher $R_c/J_{eff}(0)$ ratio indicates a shorter sequential $H_N\text{-}H_N$ distance, suggesting a preference for turn-like conformation. Although there is a noticeable decrease in the mobility of individual HN vectors (Thr33 and Ala34, Figure 6), it is apparent that the change in mobility is not significant enough to account for the increase in the R_c value of Ala 34 (Figure 7). Thus, average shorter $H_N\text{-}H_N$ distances between Thr33 and Ala34 are highly likely. Unfortunately, the $R_c/J_{eff}(0)$ value analysis is limited by the proline-rich primary sequence in this region (30-PDPTATW-36). Moreover, the corresponding $\sigma_{N\alpha}/\sigma_{\alpha N}$ ratio can not be reliably determined because of severe overlap of H^α resonances.

Region 80-83, which corresponds to the F-G turn of the folded state of Ig 18′, apparently populates turn-like conformations in 4.2 M urea. Gly82 and Glu83 have large R_c values similar to Ala34 and Trp36, which cannot be accounted for solely by a decrease in mobility in this region (Figure 7). Significant deviations from random coil values are not observed for the chemical shift deviations and the $^3J_{HNH\alpha}$ data, although this might be due to the intrinsically low sensitivity of these methods for a small population of non-random conformers. $J_{eff}(0)$, J(50 MHz) and J(450 MHz) values are similar for this region in 4.2 M and 6.0 M urea, whereas the R_c values are significantly higher in 4.2 M urea. This observation implies shorter $H_N\text{-}H_N$ distances

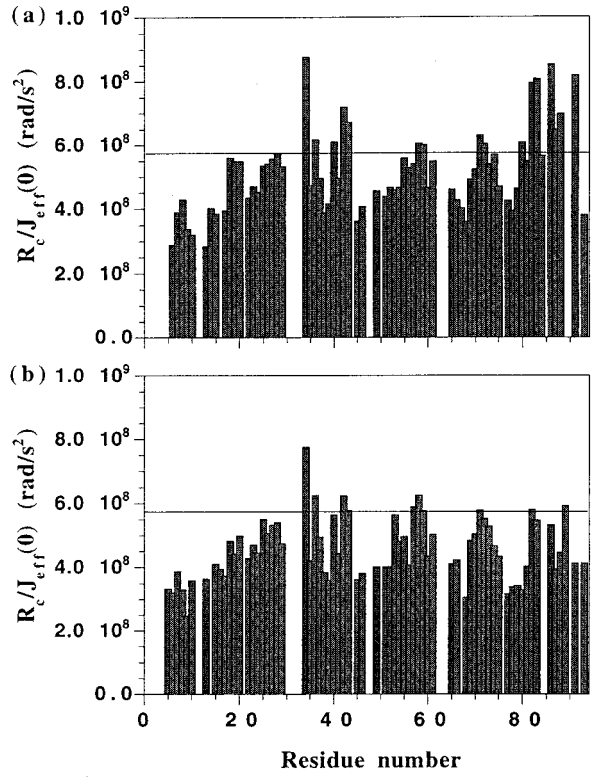

Figure 7. $R_c/J_{eff}(0)$ ratios *versus* sequence for Ig 18′ at 285 K, pH 4.9 in (a) 4.2 M urea and (b) 6.0 M urea. The value of average $R_c/J_{eff}(0)$ plus one standard deviation for the 6.0 M data is indicated by the horizontal lines in the plots.

rather than simply a change in the backbone mobility in 4.2 M urea.

As inferred from the $R_c/J_{eff}(0)$ ratios in Figure 7, region 86-92 may have preferences for turn-like structures in 4.2 M urea. The significantly lower $^3J_{HNH\alpha}$ of Ala86 is additional evidence for the preference for turn-like conformation in this region in 4.2 M urea. This region is composed of mainly hydrophobic residues (86-AIFEVIV-92). It is possible that the substantial chemical exchange observed in this region in 4.2 M urea is associated with the formation and breaking of a local hydrophobic cluster. However, no obvious correlation between the sequence-dependent hydrophobicity (Figure 8) and backbone dynamics, nor hydrophobicity and residual structures, can be observed elsewhere in the protein.

Other regions that may have turn-like structure are 40-43, 56-59 and 73-75. Although the R_c or $R_c/J_{eff}(0)$ values are not significantly increased, weak correlation between the chemical shift deviations, lower $^3J_{HNH\alpha}$ values and a noticeable increase in the $R_c/J_{eff}(0)$ ratios suggest that there may be a preference for turn-like conformations. These regions have similar structural and dynamics properties in 4.2 M and 6.0 M urea.

Leu6 has significant H^α chemical shift deviations from random coil values in 4.2 M and 6.0 M urea, and Thr7 has a marginally smaller $^3J_{HNH\alpha}$ value (−0.72 Hz) than the random coil values in 6.0 M urea. This region has average baseline $R_c/J_{eff}(0)$ ratios and undergoes fast motions on a nano- to sub-nanosecond time-scale. It is not apparent whether these deviations arise from preferential occupancy of certain conformations or other effects.

Ig 18′ is more "unfolded" in 6.0 M urea than in 4.2 M urea

In 4.2 M urea, substantial intermediate exchange processes at a rate of approximately 10^3 s^{-1} were found in the C-terminal region (84-93) of Ig 18′, which are absent when the protein is in 6.0 M urea. Presumably, in 6.0 M urea, the interconversion between different conformers in this region of the denatured state is relatively unhindered and occurs on a faster time-scale ($\gg 10^3$ s^{-1}), such that the dynamics of the C-terminal region resembles that of the N-terminal region. This suggests that the energy barrier for some exchange processes in the C-terminal region increases when the urea concentration is lowered, by a destabilisation of the transition state for exchange, or a stabilisation of some exchanging states or both. In the 4.2 M urea-denatured state, it can be assumed that this region spends relatively more time in certain conformations, presumably turn-like (as discussed above), than in the denatured state in 6.0 M urea. Together with the finding of the preference for some turn-like structures in region 80-83 in 4.2 M urea but not in 6.0 M urea, we conclude that the protein is less "unfolded", or more compact, in 4.2 M urea than in 6.0 M urea. Similar observations were made for the denatured states of an SH3 domain, in which the dynamic and NOE data indicate that a highly denatured state in 2.0 M guanidinium chloride is more unfolded than the denatured state in equilibrium with the folded state (Farrow *et al.*, 1997). Studies on staphylococcal nuclease under different denaturing conditions have also revealed a dependency of the amount of structure present in the protein on the urea concentration (Wang & Shortle, 1995).

Implication for protein folding

We have demonstrated that the structural and dynamic properties of denatured Ig 18′ can be characteristically altered when the protein is subject to different denaturant concentrations. The protein is relatively less unfolded when it is in lower denaturant concentration, and the additional structural elements detected are turn-like and undergo fast to intermediate conformational interconversions. The ^1H,^{15}N HSQC spectra of the mixture of folded and denatured states at lower urea concentrations reveal that the signals for the denatured states that are in equilibrium with the folded state more closely resemble that of the 4.2 M urea than 6.0 M urea spectra (data not

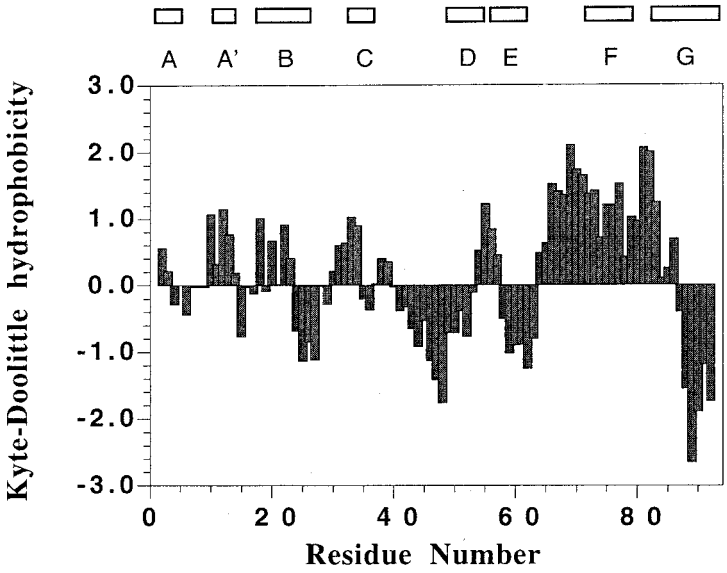

Figure 8. Kyte-Doolittle hydrophobicity *versus* sequence plot for Ig 18′. A window of 7 was used to calculate the data.

shown). A further decrease in the relative intensities of the cross-peaks for region 80-93 is observed, which suggests a further increase in motional contributions on an intermediate time-scale (micro- to millisecond) to the dynamics of this region at low denaturant concentrations. Thus, it can be inferred that the properties of the 4.2 M urea-denatured state are more similar to that of the denatured state from which protein folding is initiated. Compared to the 6.0 M urea data, additional features of the 4.2 M urea denatured state are a preference for local turn-like structures (residues 80 to 83, 86 to 92) and the enhanced restriction of local motions (residues 84 to 93). They may serve as a further means, in addition to the less denaturant-sensitive turn-like structures and motional restrictions (see Figure 9), to limit access to non-productive regions of conformational space that divert the system away from the pathway leading to the transition state of folding. We speculate that the concomitant existence of these features may be important for the initiation of folding of the protein.

Regions in the denatured states that may form non-native turn-like local structures are: 58-60, 73-75 and 86-92 (in 4.2 M urea). Non-native helical or turn structures were also found in regions corresponding to the β-strands of native states in other denatured proteins, for example, urea-denatured FK506-binding protein (Logan *et al.*, 1994), barnase (Arcus *et al.*, 1994) and barstar (Wong *et al.*, 1996). It has been reported that co-operativity and folding rate can be reduced by the presence of non-native helical structures in the denatured state of the all β-sheet α-spectrin SH3 domain (Prieto *et al.*, 1997). In barnase, region Asp93 to Tyr97 corresponding to the central β-strand of native barnase shows non-native residual structure in the denatured state and is involved in tertiary interactions in the transition state of folding. Persistent non-native local structures are likely to be a result of local interactions. Protein folding at an optimum rate requires a delicate balance between the interactions that govern the transition enthalpy and entropy of the process. Although the role of local interactions in protein folding is still unclear (Prieto *et al.*, 1997), they may help to nucleate segments of a

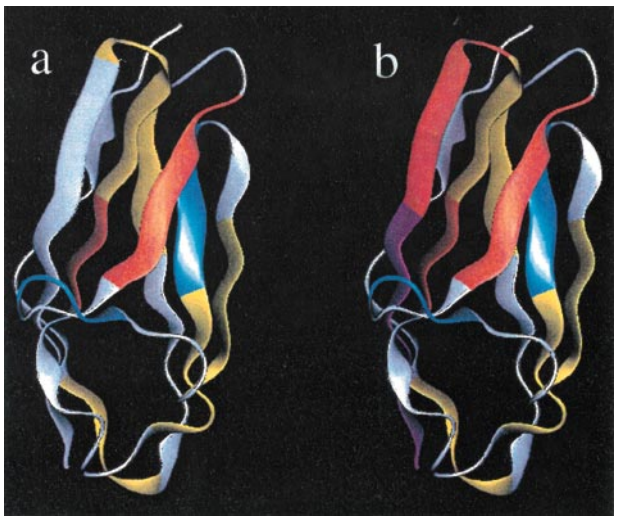

Figure 9. An illustration of structural and dynamic properties of urea-denatured Ig 18′ in 6.0 M (a) and 4.2 M (b) urea, at 285 K, pH 4.9. The N terminus is at the top and the C terminus is at the bottom. Blue indicates regions 40-43 and 56-59, which are possibly turn-like but do not have significantly high $J_{eff}(0)$; yellow indicates regions 13-16, 23-27, 49-52 and 60-64 for both a and b, 76-81 for a, 75-79 for b that have relatively high $J_{eff}(0)$; orange indicates regions 31-36 and 73-75 for both a and b, 80-83 for b, which are possibly turn-like and have relatively high $J_{eff}(0)$; red (84-85) and purple (86-92) indicate regions that have high $J_{eff}(0)$ due to significant exchange contribution to R_2, with the purple region possibly possessing turn-like structure; white indicates regions that have random coil-like structure and where no significantly high $J_{eff}(0)$ is observed.

polypeptide at the beginning of folding but have to be disrupted later (Blanco *et al*., 1997).

The role of protein dynamics in protein folding is also not well understood. In the denatured states of barnase, regions with residual structures that correspond to the initiation sites of folding, experience substantial restriction of local mobility (K. B. Wong & S.M.V.F., unpublished results). It is possible that regions with segmental compactness and/or restrictions in local mobility located in different parts of the primary sequence are involved in guiding the formation of a ''folding nucleus'' during the folding process. However, further protein engineering and kinetic studies are required to evaluate the role of these regions for the folding of this protein.

Materials and Methods

Sample preparation

Protein expression, isotopic labelling and purification of Ig 18′ were performed as described (Fong *et al*., 1996). Urea-denatured samples were prepared as follows: appropriate amounts of protein in water were concentrated to 500 µl with an Amicon Centriprep 3 at 4°C: 10 ml of a urea solution in 90% H_2O/10% ^2H_2O was prepared in a volumetric flask. The concentrated protein was rapidly dispensed and mixed into the urea solution, and the pH of the mixture was immediately adjusted to 4.95 (±0.05) at 10°C with small aliquots of 0.2 M NaOH and 0.2 M HCl. The resulting solution was concentrated to 450 µl with a Centriprep 3 at 4 ^{1}C, and the pH was readjusted to 4.95 (±0.05) at 10°C. The concentrated protein solution was centrifuged at 13000 rpm at 4°C for 30 seconds and the supernatant was collected for NMR measurements. Typical sample concentrations were about 1.4 to 1.8 mM.

NMR spectroscopy

All NMR experiments were carried out on a Bruker AMX 500 spectrometer equipped with an inverse triple resonance, single axis gradient probe. ^{1}H,^{15}N HSQC (Bodenhausen & Ruben, 1980; Kay *et al*., 1992), 3D TOCSY-HMQC (Marion *et al*., 1989) with 55 ms mixing time, 3D NOESY-HMQC (Marion *et al*., 1989) with 250 ms mixing time and 3D HSQC-NOESY-HSQC (Freund *et al*., 1996; Zhang *et al*., 1997) spectra with 250 ms mixing times were recorded with uniformly ^{15}N-labelled samples at 285 K, 4.2 M urea and 6.0 M urea concentrations respectively. The triple resonance experiments HNCO, HN(CA)CO, CBCA(CO)NH and CBCANH (Grzesiek & Bax, 1992, 1993) were recorded with a ^{15}N,^{13}C-labelled sample at 285 K, 6.0 M urea. All experiments were acquired with 1 K complex data points in the acquisition domain and sweep widths of 6024 to 8065 Hz. The sweep-width of the indirect ^{1}H dimensions in the NOESY-HMQC and TOCSY-HMQC experiments were set to the same values. The sweep-width in the ^{15}N dimension of all experiments was set to 1572 Hz. The sweep-width of the ^{13}C dimension for the CBCA(CO)NH and CBCANH was 8928 Hz, and for the HNCO and HN(CA)CO experiments 1382 Hz, respectively. Solvent suppression in some experiments was achieved by the WATERGATE sequence (Piotto *et al*., 1992). All NOESY and triple resonance experiments were acquired with echo-antiecho gradient selection and sensitivity improvement. The offset frequency in the acquisition domain was set to the water signal. The ^{15}N offset frequency was set to 116.3 ppm, carbon offset frequency was 45 ppm for the CBCANH and CBCA(CO)NH experiments, 54 ppm for the HN(CA)CO and 175 ppm for the HNCO experiments. The NOESY-HMQC and TOCSY-HMQC were acquired with 48 complex points in the ^{15}N dimension. The HN(CA)CO, HNCO were acquired with matrices of 32 (^{15}N) × 32 (^{13}C) × 1024 (^{1}H) complex points and the CBCA(CO)NH, CBCANH were acquired with matrices of 32 (^{15}N) × 58 (^{13}C) × 1024 (^{1}H) complex points. All data were processed and analysed with FELIX 2.30 (Biosym Technologies).

^{15}N R_1 ($1/T_1$), R_2 ($1/T_2$) and {^{1}H-^{15}N} NOE experiments were implemented with the incorporation of gradient selection and sensitivity improvement (Kay *et al*., 1992). The T_1 relaxation delays were set to 40, 100, 200, 300, 400, 500, 600, 700, 800, 1000 and 1200 ms. The T_2 spin echo refocussing delay time τ was set to 900µs and the relaxation times were 14, 28, 42, 56, 70, 91, 105, 126, 140, 196, 231, 266, 315 and 371 ms. Additional sets of R_2 experiments were acquired with spin-echo delays of 180µs to 2 ms. {^{1}H-^{15}N} NOEs were derived from two sets of experiments. One set consisted of a two second relaxation delay followed by a three second WALTZ16 ^{1}H decoupling. The reference experiment was acquired without ^{1}H saturation. Peak intensities extracted from the R_1 and R_2 experiments were fitted to monoexponential equations. Errors in R_1 and R_2 were estimated as the standard errors of the data fitting using KaleidaGraph (Abelbeck Software). Errors in {^{1}H-^{15}N} NOEs were estimated from the root- mean-square of noise of the spectra.

Resonance assignment of urea-denatured Ig 18′

Sequential assignment of the 6.0 M urea-denatured Ig 18′ at 285 K was achieved by the use of triple-resonance experiments. Sequential connectivities were derived from two pairs of triple resonance experiments; namely, CBCANH, CBCA(CO)NH and HN(CA)CO, HNCO (Grzesiek & Bax, 1992, 1993). Spin systems identified from CBCA(CO)NH and CBCANH were grouped according to residue types based on the $^{13}C^{\alpha}$,$^{13}C^{\beta}$ chemical shifts, and linked by matching the three sequential linkages ($^{13}C^{\alpha}$,$^{13}C^{\beta}$ and $^{13}C'$) as previously reported in the assignments of other denatured proteins (Arcus *et al*., 1994, 1995; Frank *et al*., 1995). Backbone resonances (HN, N, C′ and C$^{\alpha}$) were thus unambiguously assigned. The sequential assignment was confirmed by $d_{NN(i,i+1)}$ contacts obtained from an HSQC-NOESY-HSQC (Ikura *et al*., 1990) experiment with a 250 ms mixing time. As the ^{1}H, ^{15}N HSQC spectrum for the 4.2 M urea-denatured sample at 285 K was similar to that at 6.0 M urea, the sequential assignment of the denatured states at 4.2 M urea was achieved by $d_{NN(i,i+1)}$ connectivities obtained from HSQC-NOESY-HSQC experiments, with reference to the sequential assignment at 6.0 M urea.

Peak intensity measurements

The intensities of the NOE cross-peaks and the diagonal peaks in the 3D ^{1}H,^{15}N HSQC-NOESY-HSQC and

the 3D ^{1}H,^{15}N NOESY-HMQC spectra were measured as peak heights by a lineshape optimisation function built in FELIX 2.30 (Biosym Technologies). A Gaussian window function was applied in the ^{1}H dimensions (F1) of the NOESY experiments. The 1D vectors (^{1}H, F1) were taken from the spectra and the peak heights were optimised by fitting the lineshape of the peaks to a Gaussian function.

The intensities of the peaks in the spectra from the ^{15}N R_1, R_2 and {^{1}H-^{15}N} NOE experiments were also estimated by the peak heights. A built-in function in FELIX 2.30 for the optimisation of peak centres for 2D spectrum was employed to obtain the optimised values for the peak heights.

Reduced spectral density mapping

The frequency spectrum of rotational fluctuations of the XH bond vectors (^{15}N-^{1}H and ^{13}C-^{1}H) is described by the spectral density functions $J(\omega)$. The reduced spectral density mapping permits the direct evaluation of $J(\omega)$ for ^{15}N-^{1}H vectors at the three frequencies 0, ω_N and $\omega_H + \omega_N$. At high frequencies, the spectral density functions $J(\omega_H) \approx J(\omega_H + \omega_N) \approx J(\omega_H - \omega_N)$. Using this approximation, $J(\omega)$ at frequencies 0, ω_N and $\omega_H + \omega_N$ can be expressed in terms of the ^{15}N transverse (R_2), longitudinal (R_1) relaxation rates and heteronuclear {^{1}H-^{15}N} NOEs:

$$J_{\text{eff}}(0) = \frac{3}{2(3d+c)}\left[-\frac{1}{2}R_1 + R_2 - \frac{3}{5}R_{\text{noe}}\right] \quad (1)$$

$$J(\omega_N) = \frac{1}{3d+c}\left[R_1 - \frac{7}{5}R_{\text{noe}}\right] \quad (2)$$

$$J(\omega_H + \omega_N) = \frac{1}{5d}R_{\text{noe}} \quad (3)$$

where:

$$R_{\text{noe}} = (\{^1H - ^{15}N\}NOE - 1)R_1\frac{\gamma_N}{\gamma_H} \quad (4)$$

and $d = \gamma_H^2\gamma_N^2(h/2\pi)^2/4r_{HN}^6$, $c = \Delta^2\omega_N^2/3$; Δ is the chemical shift anisotropy of the amide nitrogen atom; γ_H and γ_N are the gyromagnetic ratios for ^{1}H and ^{15}N nuclei respectively; h is the Planck's constant; r_{HN} is the NH bond length. For $r_{HN} = 1.02$ Å and $\Delta = -160$ ppm, d is approximately equal to 1.3 x 10^9 (rad/seconds)^2 and the constant c is approximately equal to 0.87×10^9 (rad/seconds)^2 at 11.74 T (Peng & Wagner, 1994). $J_{\text{eff}}(0)$ is used to denote that contributions from chemical exchange and other pseudo first-order processes (R_{ex}) to R_2 are not considered explicitly in the calculation. Thus, an increase in $J_{\text{eff}}(0)$ can be caused by a relatively slower rotational fluctuation of the ^{15}N-^{1}H vector on a ns time scale and/or pseudo first-order processes that occur on a micro- to millisecond time-scale. In either case, for highly flexible denatured states, it indicates that some motional restriction mechanisms are contributing to the reorientation of the ^{15}N-^{1}H vector.

Standard deviations for the calculation of the spectral density functions were estimated by Monte Carlo simulation: 10,000 input data sets were generated randomly from a normal distribution of R_1, R_2 and {^{1}H-^{15}N} NOEs with the standard errors of the raw data as standard deviations. These data were used to simulate the statistical distributions of $J_{\text{eff}}(0)$, $J(\omega_N)$ and $J(\omega_H + \omega_N)$.

Estimation of R_c

Cross-relaxation rates, R_c , are estimated according to:

$$R_c = (1/t_m)\ln[(1 + \sigma_{NN})/(1 - \sigma_{NN})] \quad (5)$$

where t_m is the mixing time of the NOESY experiment; σ_{NN} is the experimental intensity ratio of H_N-H_N NOE cross-peak to diagonal peak. Alternatively, R_c can be expressed as:

$$R_c = 0.2\gamma^4(h/2\pi)^2(\mu_0/4\pi)^2Jr^{-6} \quad (6)$$

where γ is the gyromagnetic ratio for hydrogen, h is the Planck's constant, μ_0 is the permeability of free space; $J = |6\ J(2\omega_H) - J(0)|$, where $J(0)$ and $J(2\omega_H)$ are the spectral density functions at frequencies 0 and $2\omega_H$, respectively; and r is the population averaged H_N-H_N distance.

Acknowledgements

S.F. is supported by a Croucher Foundation Scholarship, Hong Kong.

References

Arcus, V. L., Vuilleumier, S., Freund, S. M. V. & Bycroft, M. (1994). Toward solving the folding pathway of barnase: the complete backbone ^{13}C,^{15}N, and ^{1}H NMR assignment of its pH-denatured state. *Proc. Natl Acad. Sci. USA,* **91**, 9412–9416.

Arcus, V. L., Vuilleumier, S., Freund, S. M. V., Bycroft, M. & Fersht, A. R. (1995). A comparison of the pH-, urea-, and temperature-denatured states of barnase by heteronuclear NMR: implications for the initiation of protein folding. *J. Mol. Biol.* **254**, 305–321.

Barun, D., Wider, G. & Wüthrich, K. (1994). Sequence corrected ^{15}N ''random coil'' chemical shifts. *J. Am. Chem. Soc.* **116**, 8466–8469.

Bax, A. & Grzesiek, S. (1993). Methodological advances in protein NMR. *Acc. Chem. Res.* **26**, 131–138.

Blanco, F. J., Ortiz, A. R. & Serrano, L. (1997). Role of a nonnative interaction in the folding of the protein G B1 domain as inferred from the conformational analysis of the alpha-helix fragment. *Folding Des.* **2**, 123–133.

Bodenhausen, G. & Ruben, D. L. (1980). Natural abundance nitrogen-15 NMR by enhanced heteronuclear spectroscopy. *Chem. Phys. Letters*, **69**, 185–188.

Carlsson, U. & Jonsson, B.-H. (1995). Folding of β-sheet proteins. *Curr. Opin. Struct. Biol.* **5**, 482–487.

Dill, K. A., Fiebig, K. M. & Chan, H. S. (1993). Cooperativity in protein-folding kinetics. *Proc. Natl Acad. Sci. USA,* **90**, 1942–1946.

Dobson, C. M. (1992). Unfolded proteins, compact states and molten globules. *Curr. Opin. Struct. Biol.* **2**, 6–12.

Esposito, G. & Pastore, A. (1988). An alternative method for distance evaluation from NOESY spectra. *J. Magn. Reson.* **76**, 331–336.

Farrow, N. A., Zhang, O., Forman-Kay, J. D. & Kay, L. E. (1995). Comparison of the backbone dynamics of a folded and an unfolded SH3 domain existing in equilibrium in aqueous buffers. *Biochemistry,* **34**, 868–878.

Farrow, N. A., Zhang, O., Forman-Kay, J. D. & Kay, L. E. (1997). Characterization of the backbone

dynamics of folded and denatured states of an SH3 domain. *Biochemistry*, **36**, 2390–2402.
Finkelstein, A. V. (1991). Rate of β-structure formation in polypeptides. *Proteins: Struct. Funct. Genet.* **9**, 23–27.
Fong, S., Hamill, S. J., Proctor, M., Freund, S. M. V., Benian, G. M., Chothia, C., Bycroft, M. & Clarke, J. (1996). Structure and stability of an immunoglobulin superfamily domain from twitchin, a muscle protein of the nematode *Caenorhabditis elegans*. *J. Mol. Biol.* **264**, 624–639.
Frank, M. K., Clore, G. M. & Gronenborn, A. M. (1995). Structural and dynamic characterisation of the urea denatured state of the immunoglobulin binding domain of streptococcal protein by mutidimensional heteronuclear NMR spectroscopy. *Protein Sci.* **4**, 2605–2615.
Freund, S. M. V., Wong, K. B. & Fersht, A. R. (1996). Initiation sites of protein folding by NMR analysis. *Proc. Natl Acad. Sci. USA*, **93**, 10600–10603.
Grzesiek, S. & Bax, A. (1992). Improved 3D triple-resonance NMR techniques applied to a 31 kDa protein. *J. Magn. Reson.* **96**, 432–440.
Grzesiek, S. & Bax, A. (1993). Amino-acid type determination in the sequential assignment procedure of uniformly C-13/N15–enriched proteins. *J. Biomol. NMR*, **3**, 185–204.
Ikura, M., Bax, A., Clore, G. M. & Gronenborn, A. M. (1990). Detection of nuclear overhauser effects between degenerate amide proton resonances by heteronuclear 3-dimensional nuclear-magnetic-resonance spectroscopy. *J. Am. Chem. Soc.* **112**, 9020–9022.
Ishima, R. & Nagayama, K. (1995). Protein backbone dynamics revealed by quasi spectral density function analysis of amide N-15 nuclei. *Biochemistry*, **34**, 3162–3171.
Kay, L. E. (1997). NMR methods for the study of protein structure and dynamics. *Biochem. Cell Biol.* **75**, 1–15.
Kay, L. E., Torchia, D. A. & Bax, A. (1989). Backbone dynamics of proteins as studied by ^{15}N inverse detected heteronuclear NMR spectroscopy: application to staphylococcal nuclease. *Biochemistry*, **28**, 8972–8979.
Kay, L. E., Keifer, P. & Saarinen, T. (1992). Pure absorption gradient enhanced heteronuclear single quantum correlation spectroscopy with improved sensitivity. *J. Am. Chem. Soc.* **114**, 10663–10665.
Logan, T. M., Thériault, Y. & Fesik, S. W. (1994). Structural characterisation of the FK506 binding protein unfolded in urea and guanidine hydrochloride. *J. Mol. Biol.* **236**, 637–648.
Macura, S. & Ernst, R. R. (1980). Elucidation of cross relaxation in liquids by two-dimensional NMR spectroscopy. *Mol. Phys.* **41**, 95–117.
Marion, D., Driscoll, P. C., Kay, L. E., Wingfield, P. T., Bax, A., Gronenborn, A. M. & Clore, G. M. (1989). Overcoming the overlap problem in the assignment of ^{1}H NMR spectra of larger proteins by use of three-dimensional heteronuclear ^{1}H-^{15}N Hartmann-Hahn-multiple quantum coherence and nuclear Overhauser-multiple quantum coherence spectroscopy. Application to interleukin 1β. *Biochemistry*, **28**, 6150–6156.
Matouschek, A., Serrano, L., Meiering, E. M., Bycroft, M. & Fersht, A. R. (1992). The folding of an enzyme. 5. H/^{2}H exchange nuclear magnetic resonance studies of the folding pathway of barnase–complementary to and agreement with protein engineering studies. *J. Mol. Biol.* **224**, 837–845.
Merutka, G., Dyson, H. J. & Wright, P. E. (1995). Random coil H-1 chemical-shifts obtained as a function of temperature and trifluoroethanol concentration for the peptide series GGXGG. *J. Biomol. NMR*, **5**, 14–24.
Moult, J. & Unger, R. (1991). An analysis of protein folding pathways. *Biochemistry*, **30**, 3816–3824.
Neri, D., Billeter, M., Wider, G. & Wüthrich, K. (1992). NMR determination of residual structure in a urea-denatured protein, the 434-repressor. *Science*, **257**, 1559–1563.
Nölting, B., Golbik, R., Neira, J. L., Soler-Gonzalez, A. S., Schreiber, G. & Fersht, A. R. (1997). The folding pathway of a protein at high resolution from microseconds to seconds. *Proc. Natl Acad. Sci. USA*, **94**, 826–830.
Peng, J. W. & Wagner, G. (1992a). Mapping of spectral density-functions using heteronuclear NMR relaxation measurements. *J. Magn. Reson.* **98**, 308–332.
Peng, J. W. & Wagner, G. (1992b). Mapping of the spectral densities of N-H bond motions in Eglin-c using heteronuclear relaxation experiments. *Biochemistry*, **31**, 8571–8586.
Peng, J. W. & Wagner, G. (1994). Investigation of protein motions via relaxation measurements. *Methods Enzymol.* **239**, 563–596.
Peng, J. W. & Wagner, G. (1995). Frequency spectrum of NH bonds in eglin c from spectral density mapping at multiple fields. *Biochemistry*, **34**, 16733–16752.
Piotto, M., Saudek, V. & Sklenar, V. (1992). Gradient-tailored excitation for single-quantum NMR spectroscopy of acqueous solutions. *J. Biomol. NMR*, **2**, 661–665.
Prieto, J., Wilmans, M., Jiménez, M. A., Rico, M. & Serrano, L. (1997). Non-native local interactions in protein folding and stability: introducing a helical tendency in the all beta-sheet alpha-spectrin SH3 domain. *J. Mol. Biol.* **268**, 760–778.
Radford, S. E., Buck, M., D., T. K., Dobson, C. M. & Evans, P. A. (1992). Hydrogen exchange in native and denatured states of hen egg-white lysozyme. *Proteins: Struct. Funct. Genet.* **14**, 237–248.
Roder, H. (1989). Structural characterisation of protein folding intermediates by proton magnetic resonance and hydrogen exchange. *Methods Enzymol.* **176**, 446–473.
Saulitis, J. & Liepins, E. (1990). Quantitative evaluation of interproton distances in peptides by two-dimensional Overhauser effect spectroscopy. *J. Magn. Reson.* **87**, 80–91.
Schönbrunner, N., Pappenberger, G., Scharf, M., Engels, J. & Kiefhaber, T. (1997). Effect of preformed correct tertiary interactions on rapid two-state tendamistat folding: evidence for hairpins as initiation sites for β-sheet formation. *Biochemistry*, **36**, 9057–9065.
Serrano, L., Matouschek, A. & Fersht, A. R. (1992). The folding of an enzyme. 6. The folding pathway of barnase–comparison with theoretical models. *J. Mol. Biol.* **224**, 847–859.
Shortle, D. (1993). Denatured states of proteins and their roles in folding and stability. *Curr. Opin. Struct. Biol.* **3**, 66–74.
Shortle, D. (1996a). The denatured state (the other half of the folding equation) and its role in protein stability. *FASEB J.* **10**, 27–34.

Shortle, D. (1996b). Structural-analysis of nonnative states of proteins by NMR methods. *Curr. Opin. Struct. Biol.* **6**, 24–30.

Smith, L. J., Bolin, K. A., Schwalbe, H., MacArthur, M. W., Thornton, J. M. & Dobson, C. M. (1996). Analysis of main-chain torsion angles in proteins: prediction of NMR coupling constants for native and random coil conformations. *J. Mol. Biol.* **255**, 494–506.

Stonehouse, J. & Keeler, J. (1995). A convenient and accurate method for the measurement of the values of spin-spin coupling-constants. *J. Magn. Reson.* **112**, 43–47.

Varley, P., Gronenborn, A. M., Christensen, H., Wingfield, P. T., Pain, R. H. & Clore, G. M. (1993). Kinetics of folding of the all-β sheet protein interleukin-1β. *Science,* **260**, 1110–1113.

Wang, Y. & Shortle, D. (1995). The equilibrium folding pathway of staphylococcal nuclease: identification of the most stable chain-chain interactions by NMR and CD spectroscopy. *Biochemistry,* **34**, 15895–15905.

Wishart, D. S., Bigham, C. G., Holm, A., Hodges, R. S. & Sykes, B. D. (1995). ^{1}H,^{13}C and ^{15}N random coil NMR chemical shifts of the common acids. I. Investigations of nearest-neighbour effects. *J. Biomol. NMR,* **5**, 67–81.

Wong, K. B., Freund, S. M. V. & Fersht, A. R. (1996). Cold denaturation of Barstar: ^{1}H,^{15}N and ^{13}C NMR assignment and characterisation of residual structure. *J. Mol. Biol.* **259**, 805–818.

Wüthrich, K. (1994). NMR assignment as a basis for structural characterisation of denatured states of globular-proteins. *Curr. Opin. Struct. Biol.* **4**, 93–99.

Zhang, O. W., Forman-Kay, J. D., Shortle, D. & Kay, L. E. (1997). Triple-resonance NOESY-based experiments with improved spectral resolution: applications to structural characterisation of unfolded, partially folded and folded proteins. *J. Biomol. NMR,* **9**, 181–200.

Edited by P. E. Wright

(Received 21 November 1997; received in revised form 2 February 1998; accepted 4 February 1998)

http://www.hbuk.co.uk/jmb

Supplementary material comprising two Tables of resonance assignments is available from JMB Online